Lasers in Manufacturing Conference 2015

Hydrodynamic instabilities and ablation phenomena under the laser melting of powder layer

Yuri Chivel*

Merphotonics, 42100 Saint Etienne , France

Abstract

Process of melting of the thick metal powder layers was investigated under temperature control. Ejection of dispersed particles from the overheated melt has been observed and investigated. Mechanisms of the melt penetration into loose powder bed have been determined. Instability of the contact surface between the melt and powder revealed by in experiment has been studied. Numerical simulation of the Rayleigh - Taylor instability suggest that instability develops starting from small scale passing to the large-scale structure

Keywords: selective laser melting; temperature monitoring; instability, thermal conductivity; ablation; droplet ejection.

1.Introduction

Selective laser melting is one of methods to produce complex 3D objects, under the general category of additive manufacturing To reproduce the shape of the part laser beam melts powder material layer by layer. Solidifying track by track, layer by layer, the 3D part with required geometry is created.

The ejected liquid droplets can be seen during the melting process (fig.1) in many cases. This is not considered as a deviation from the technological regime and it is perceived as inevitable. But it is not so. Particulate emissions lead to defects in the layers, the outer surface geometry violations and may even cause damage of the power optics because the particles have velocities of several meters per second.

* Corresponding author. Tel.: +330953009245.
E-mail address: yuri.chivel@gmail.com.

In addition some instabilities of the melting process also lead to defects and catastrophic decline in the accuracy and quality of products. The study of these phenomena and the selection of optimum regimes of melting is a very urgent task.

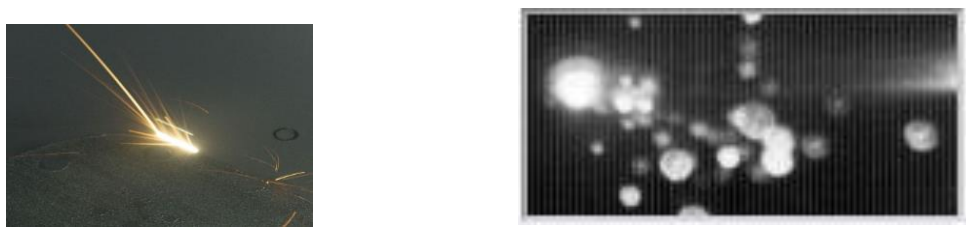

a b

Fig. 1 Images of SLM process in visible (a) and infrared (b): integral (a) , (b) high-speed shooting (Smurov , 2009)

2.Experimental

2.1 Optical monitoring of the melting process

Study of the melting process was carried out with the use of special methods of measurement and instrumentation. The principles of measuring the surface temperature of powder bed in the focal spot of the laser radiation while scanning the surface using galvanoscanner with F-teta lens have been elaborated (Chivel, 2012) (fig.2 b). Measurements are carried out at wavelengths close to laser wavelength (fig.1b) which are prominent using a gradient type dichroic mirrors and filters (fig.1a). Special optical schemes was designed. A two-wavelength pyrometer (fig.2a) with time resolution 50μs and spatial resolution 50 μm based on two InGaAs photodiodes registers the surface thermal radiation on two wavelengths in the range 900-1200 nm. The image of scanning area with diameter 130 μm is rendered on fiber diaphragm 8, diameter of which 100 μm fixes the area of signal integratio

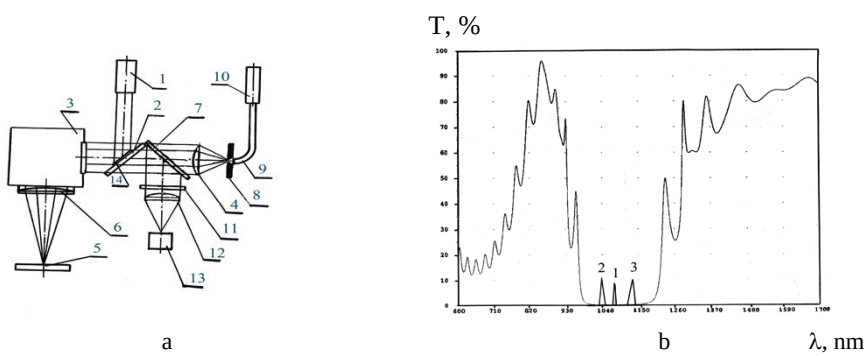

Fig.2 (a)- Scheme of temperature measurements: 1- laser, 2- gradient mirror, 3- scan head, 4- lens, 6- F-teta lens, 5- powder bed, 7- dichroic mirror, 8- lens, 9-fiber, 10 – pyrometer, 11- filter, 12 – lens, 13- CCD.(b)- Transmisivity of the scanner mirror. 1 – laser line ; 2 , 3 – lines of thermal radiation separated by filters.

The monitoring of the temperature distribution in laser irradiation zone is based on high speed digital CCD – camera (pos.13). The image of the melting zone is projected onto the matrix plane of digital CCD camera through interference filter at 850 нм and spatial brightness temperature distribution is determined. As the maximum colour temperature have been valued by pyrometry it is possible to have colour temperature distribution from brightness temperature distribution. The signal from pyrometer and CCD camera was processed by a special software developed in MerPhotonics.

The calibration of the optical system was performed by tungsten halogen lamp as a secondary source with a transmitting diffuser diameter of 1mm. The lamp, in turn, was calibrated by a precision blackbody source. For 1800 K temperature maximum error was about ± 10 K.

2.2 Experimental conditions of the SLM process

SLM experiments were carried out using single-mode continuous-wave Ytterbium fiber laser operating at 1075 nm wavelength (IPG Photonics Corp.). The laser beam had a TEM_{00} Gaussian profile, 70 μmspot size, and 200 W maximum power. Argon and nitrogen was used as a protective atmosphere in all experiments.

In these experiments, a some layer of Cu (25-50 μm), CoCr and 316 steel powder was used. The thickness of the powder bed was 3 mm. **L**ayers were scanned with scan shift 30 μm which ensured the creation of a thin layer of the melt. Only one cross- section 100 x 100 mm^2 was scanned with the scan speed 100 mm/s.

3. Results and discussions

3.1 Ablation with droplets ejection.

Ejection of droplets from the overheated melt has been investigated. Formation of the molten layer leads to a transition of the porous structure into the melt , gas heating in the pores and explosive like destruction the porous structure with the droplets release.

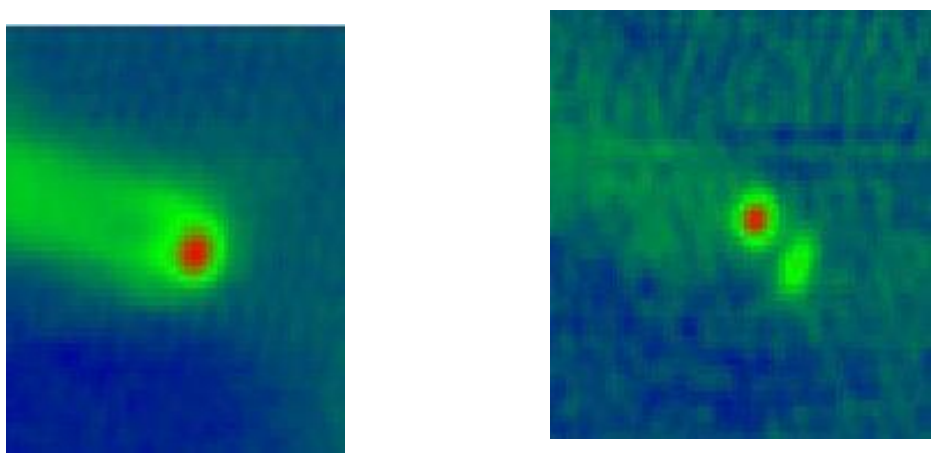

a b

Fig. 3 Images of the melting process when scanning without droplet release (a) and with one (b). Powder CoCr . P= 80W –(a) , P= 50W –(b). Scan speed – 100 mm/s.

Found that droplets ejection goes sides-and-forth relative to motion of the laser focal spot when scanning

(fig.3,4). Temperature measurements showed that the droplet temperature is close to the melt temperature (Fig. 4). When the melt temperature in the laser spot is equal 2000 K, the ejected droplet temperature reaches 1850 K.

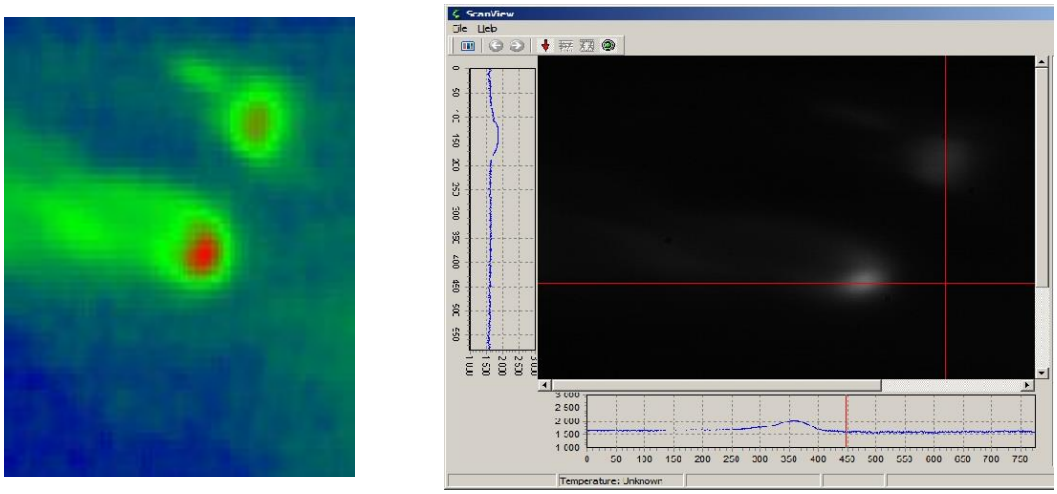

a b

Fig. 4 Image of the melting process when scanning with droplet release (a). Powder CoCr . P= 80W –(a) , P= 50W – (b). Scan speed – 100 mm/s. Temperature distributions in laser spot and on the droplet surface.

Droplets reach the velocity of 1 - 2 m / s at a size of 10-100 μm.

On the surface of the powder layer after melting can be observed heterogeneity and discontinuities. Discontinuities can be caused either by a finite merging time of melted powder particles or gas jets escaping from pores during powder heating. The importance of the latter process during processing even solids was pointed out in paper (Chivel , 2001).

An intensive gas desorption takes place when the pores surface is heated up to 2000 K (Chivel et al. ,2007). The gas filled in pores, heats up to pores wall temperature through thermal conductivity in a short time to 10^{-8} s. The pressure about 10–100 MPa, developed by gas, could result in melt surface destruction. The destruction can occur in the solid state when the gas pressure in the pores exceeds the damage threshold of the material, or in the liquid state as the results of gas bubbles growth. Droplet emissions facilitated by melt overheating due to the fall in its viscosity.

Pressure of the desorbed and heated gas in the pores was calculated from relationships [3]:

$$R(0) = R_0;\quad \left(\frac{dR}{dt}\right)_{t=0} = 0;\ P(0) = \frac{3(\gamma-1)Cv\cdot A\cdot m\cdot T_0}{R_0};$$
$$\left(\frac{dP}{dt}\right)_{t=0} = \frac{3(\gamma-1)Cv\cdot A\cdot m\cdot B}{R_0} \qquad (1)$$

where R- pore radius, P - gas pressure, γ - the specific heats ratio, Cv - the gas specific heat, B - the heating rate, T_0 - the liberated gas temperature,m is gas molecular mass, R_0 - the initial bubble radius, A - surface

density of the absorbed gas.

For the pore radius equal to 10 μm the maximum pore gas pressure at 2000 K is ~ 10 MPa .

It should be noted that the transfer of SLM process in vacuum conditions minimizes droplets ejection as observed under electron-beam melting using equipment of the firm ARCAM.

3.2 Hydrodynamic instabilities of the SLM process

As was apparent after experiments that due to the high thermal conductivity of copper and the low velocity of the transverse scan movement of track the front of melting moves directly ahead of the laser track (fig.5). Accumulation of heat in the layer causes their overheating and affects the flow of the melting process, encouraging the development of the instability of the contact surface between the melt and powder (Chivel , 2013) in a gravity field - Rayleigh - Taylor (RT) instability (Chandrasekhar, 1959).

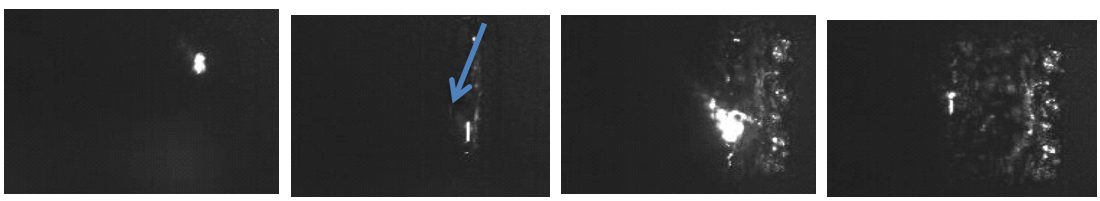

Fig. 5. Overhang layer melting. Frame recording : Cu powder with CuO coating. Exposure time - 0.01 s , 78 fps. Arrow-melting front.

Observed structures on the contact surface between melt and powder (fig.6 a,b) are typical of the Rayleigh - Taylor instability. The main factors holding back the development of instability– viscosity and time. But at 2000K viscosity of copper melt is only 10^{-3} Pa·s , cooling rate of the melt 10^{-3} K/s (Lisenko et al.,2008) and the characteristic time of the penetration of the melt in the powder bed can be estimated fromt he characteristic time of entry of spherical bodies ~ 0.1s [8] which is consistent with the measured time of growth of structures on the surface (Fig.5)**.**

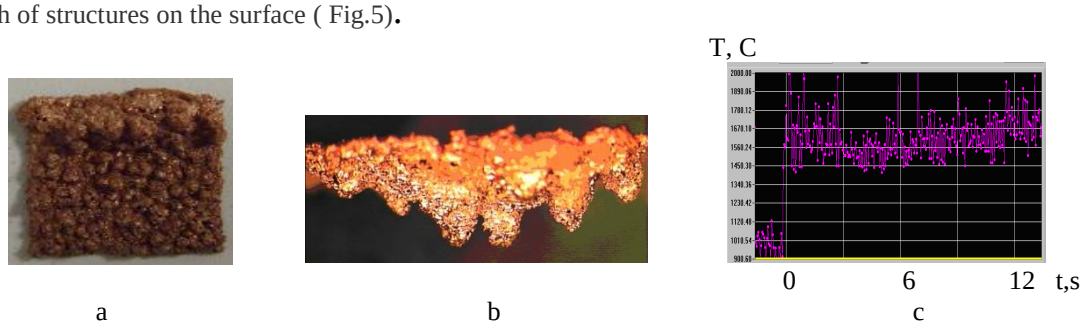

Fig. 6. Structure of overhang layer. (a) – bottom view, (b) – end view , (c,d) – Brightness temperatures in melted area : (c) - Pyrometer data.Powder – Cu, 25-50 μm, P = 80W.

3.3 Rayleigh Taylor instability modelling

Numerical simulation of the Rayleigh Taylor instability at the interface between the melt and the layer thickness of 4mm copper powder 20-40 in diameter which was considered as a liquid with a certain density and viscosity has been conducted. ProgramSOLA-VOF (Nichols et al.,1980) has been used for modeling the

motion of an incompressible viscous fluid taking into account heat conduction (Antonova et al.,2011). Characteristics of the materials used in the calculation shown in Table 1.

Table 1

	air	***melt***	***powder***
$\rho[kg/m^3]$	*0.17*	*8600*	*4300*
$C_p[/kg\times K]$	*1006*	*380*	*190*
$k[w/m\times K]$	*0.0242*	*380*	*1*
$n[kg/m\times s]$	*$3*10^{-5}$*	*0.002*	*0.1-1*

Temperature of the melt layer thickness of 0,5 mm was assumed to be 2200K. At this temperature, the dynamic viscosity of the molten copper is 2 10^{-3} Pa·s. The viscosity of the powder was calculated from the dependence obtained for the viscosity of the powder bed when lowering a ball diameter D in powder bed (De Brugne ,et al.,2004):

$$\eta = \mu \cdot g^{0.5} (\rho_m \cdot \rho_g)^{0,5} \cdot D^{1,5} / (1- p/p_c) \qquad (2)$$

where $\mu = tg\alpha$, α - angle of repose, D - characteristic size of the structures of RT instability, ρ_m , ρ_g - melt density and density of the powder bed, p and p_c – packing fraction of powder bed and critical packing fraction when $\eta = \infty$(taken to be 0,66 according [9]). As seen from (2) the powder viscosity depends on the size of the penetrating body and for D = 1 mm is 5 Pa· s,but for D = 0.3 mm is 0.5 Pa·s. For comparison, the viscosity of fuel - oil - 3 Pa·s. The results of modeling are presented at Fig. 7,8.

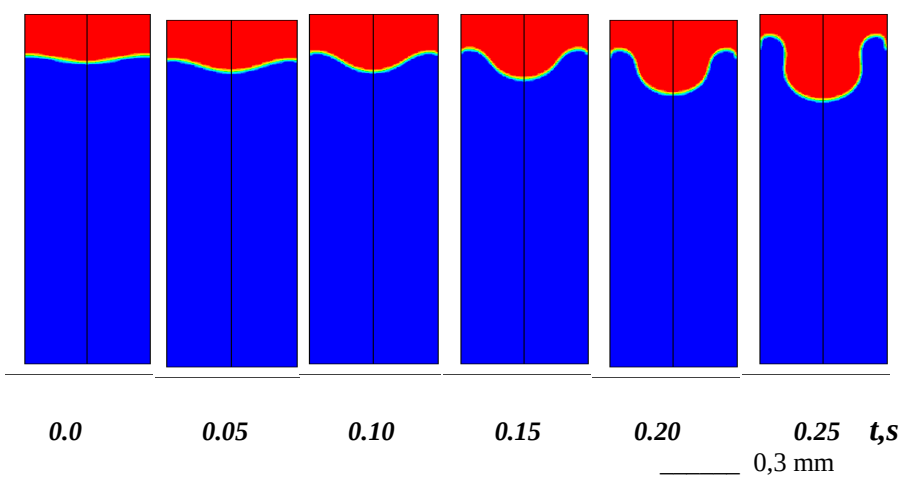

Fig.7 The development of Rayleigh Taylor instability for 0,3 mm mode, viscosity of powder – 0.5 Pa s.
Calculations showed that at least two orders of magnitude time penetration of the melt into the pores of the powder exceeds the time of large-scale instabilities. This substantiated of continuum model.

Despite the high viscosity instability develops starting from small scale as observed experimentally(Fig. 6 a) passing to the large-scale structure -1mm (Fig.6 b).

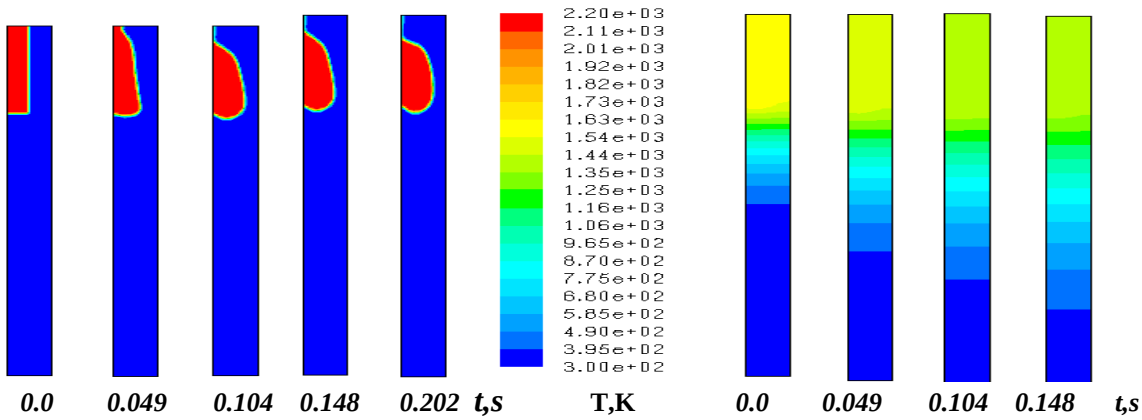

Fig. 8 The development of Rayleigh Taylor instability for 0.13 mm width melt, obtained after the first pass of the laser spot (viscosity of powder – 0.5 Pa s.)

Calculation of instability and the heat propagation is carried out for a two-phase medium contained in a rigid box with adiabatic walls, width 0.26 mm and a height of 4 mm. The melt occupies the upper left corner (Fig. 8) dimensioned 0.13x1 mm, and heated up to 2200 K, the rest region - powder at a temperature of 300 K. Start time conventionally corresponds to a situation that is realized after the first pass, the shift of 30 microns and top movement in the opposite direction, the laser beam width of 100 microns. The instant powder is melted in the area of 130 mm width and the melt acquired a twice smaller volume. Further, under the influence of gravity melt falls in the powder. The figure 8 show that in 0.03 seconds melt is converted into droplets. According the simulation results, inclusions of the solidified droplets with size about 1 mm should be observed in experiment.

3.4 Influence of instability on SLM process

Emerged on the surface structures because of the instability (fig. 6) have high absorptivity due to multiple reflections ofthe laser radiation in the pits (fig.9 a,b). The result is the rise of surface temperature in these areas. High temperature fluctuations are observed during ~3s (fig. 6 c).

Fig. 9. Instabilitie of the melting process : (a)- frame recording, 1 – melt front; (b) - cross-section, (c) - spatial temperature distribution,

When scanning a loose powder bed from powders of CoCr, steel 316 with low thermal conductivity and higher absorptivity the melt front did not overtake the scan track.Instabilities also are seen but in most cases at the border of the scan area where scan spot is stopped and overheating takes place.

The second mechanism of melt instabilities and super-deep penetration of the laser radiation in a powder bed is associated with balling effect. Large drops of melt draw nearby powder (Fig.10) with resulting laser radiation penetration to powder bed at a depth up to 2 mm.

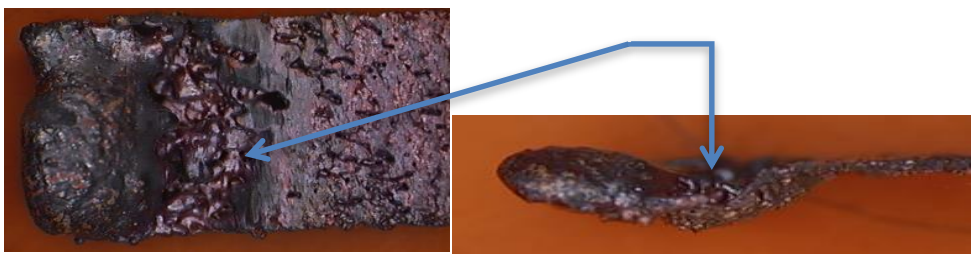

a _____ 5 mm b

Fig. 10 Surface structure resulting from the balling effect .a – top view , b – side view. Cu, P=89W.

3.5 Optimal regime of 3 D object selective laser melting process

Direct temperature measurements during the selective laser melting process of the 3D object from steel 316L powder have been conducted. In these experiments, a layers of 50 µm thickness of 20 µm powder in diameter were scanned with velocity 100 mm/s and shift 120 µm. All layers were scanned doubly. Temperature measurements during all process showed that brightness temperature in the focal spot 100 µm in diameter did not exceed 1800-1900K (Fig.10), significantly below the theoretically predicted [12].

Maximum brightness temperature at first and second scan differ little in value (Fig .10). Droplets ejection were not observed during the entire process of sintering of the object. This mode of SLM process can be considered as optimum.

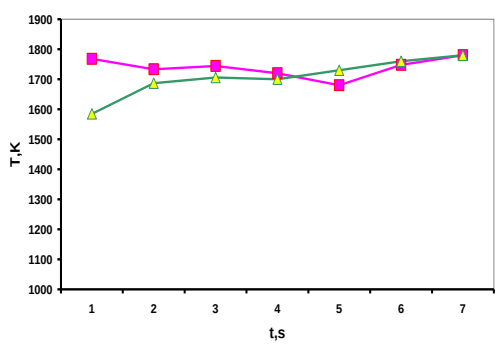

Fig. 11 Optimal regime of the selective melting : Maximum melt temperature in focal spot : □ – first scan , Δ - second scan. 316L steel powder.

4.Conclusion

Research of the ablation processes at SLM showed that droplets ejection are caused by layer porous structure, its gas-filled and melt viscosity decrease when the melt overheating.

It was determined that the destruction of thick powder layer is associated with a overheating and with the emergence of instabilities and their growth.

At first experimentally the development of Rayleigh Taylor instability of the interface between the liquid (melt) and granular (powder) media has been set.

The mechanisms of the melt penetration into loose powder bed have been determined:

Accumulation of heat in the molten thick layer results in the development of the instability of the contact surface between the melt and loose powder in a gravity field - Rayleigh - Taylor (RT) instability. RT instability progress under laser radiation action causes the complete loss of stability of the molten layer with a dip to the loose powder bed.

The second mechanism of super-deep penetration of laser radiation in a powder bed has associated with balling effect. Large drops of melt draw nearby powder with resulting laser radiation penetration to a depth up to 2-3 mm.

Direct temperature measurements during the selective laser melting process of the 3D object made it possible to determine the optimal conditions for the melting of the powder layer without release of droplets. Optimal conditions of selective melting without droplet release are in the temperature range slightly above the melting point of the powder material .

References

Smurov I. , Laser processes optical sensing and control,2007, Proc. LIM, p. 363.

Chivel, Yu., Method and device for measuring the surface brightness and colour temperature in the area of the laser irradiation, 2012, Patent № 201107, EP Application № 12831885.

Chivel Yu. 2001, Model of laser induced ablation of solids, Proc. SPIE, 4423,p.232-237.

Chivel Yu., Petrushina M., Smurov I., 2007, Influence of initial micro-porosity of target on material ejection under nanosecond laser pulses, Appl. Surf. Sci. , 254, p.816- 820.

Chivel Yu. 2013, On-line temperature monitoring of the selective laser melting , Physics Procedia , 41, pp. 897 – 903.

Chandracekhar S., 1961,Hydrodynamic and Hydromagnetic Stability, Oxford Press, p.505.

Lisenko A.,Borisov G.: 2008,Peculiarities of metal crystallization, Physics of metal and metallurgy, 105, p.451.

YohannesB.,Hill K.,Khazanovich L.:, 2009,Mechanistic modeling of unbound granular materials , Final Report, Univ. Minnesota, p.18.

Nichols B.D., Hirt C.W., Hotchkiss R.S., 1980, SOLA-VOF : A solution algorithm for transient fluid flow with multiple free boundaries, Los Alamos Sci. Lab. Report LA-8355,Los Alamos.

Antonova L.I., Gladuch G.G., Glova A.F., Drobyazko S.V., Krasukov A.G., Rerih V.K., Taran M.D. , 2011, Removal of water from a shallow bath under the influence of the laser pulse, Quantum Electronics , 41, p.453.

De Brugn J.R., Walsh A.M. ,2004, Penetration of sphere into loose granular media, Canadian Journ.Phys.,82, p.430.